Nuclear Factor-κB Signature of Inflammatory Breast Cancer by cDNA Microarray Validated by Quantitative Real-time Reverse Transcription-PCR, Immunohistochemistry, and Nuclear Factor-κB DNA-Binding

Steven J. Van Laere,[1] Ilse Van der Auwera,[1] Gert G. Van den Eynden,[1] Hilde J. Elst,[1] Joost Weyler,[2] Adrian L. Harris,[3] Peter van Dam,[1] Eric A. Van Marck,[1] Peter B. Vermeulen,[1] and Luc Y. Dirix[1]

Abstract

Purpose: Inflammatory breast cancer (IBC) is the most aggressive form of locally advanced breast cancer with high metastatic potential. In a previous study, we showed that IBC is a different form of breast cancer compared with non-IBC by cDNA microarray analysis. A list of 756 genes with significant expression differences between IBC and non-IBC was identified. In-depth functional analysis revealed the presence of a high number of nuclear factor-κB (NF-κB) target genes with elevated expression in IBC versus non-IBC. This led to the hypothesis that NF-κB contributes to the phenotype of IBC. The aim of the present study was to further investigate the role of NF-κB in IBC.

Experimental Design: Immunohistochemistry and NF-κB DNA-binding experiments were done for all NF-κB subunits (RelA, RelB, cRel, NFkB1, and NFkB2) using IBC and non-IBC specimens. Transcriptionally active NF-κB dimers were identified by means of coexpression analysis. In addition, quantitative real-time reverse transcription-PCR for eight NF-κB target genes, selected upon a significant, 3-fold gene expression difference between IBC and non-IBC by cDNA microarray analysis, was done.

Results: We found a significant overexpression for all of eight selected NF-κB target genes in IBC compared with non-IBC by quantitative real-time reverse transcription-PCR. In addition, we found a statistically elevated number of immunostained nuclei in IBC compared with non-IBC for RelB ($P = 0.038$) and NFkB1 ($P < 0.001$). Immunohistochemical data were further validated by NF-κB DNA-binding experiments. Significant correlations between immunohistochemical data and NF-κB DNA binding for RelA, RelB, NFkB1, and NFkB2 were found. Transcriptionally active NF-κB dimers, composed of specific combinations of NF-κB family members, were found in 19 of 44 IBC specimens compared with 2 of 45 non-IBC specimens ($P < 0.001$). In addition, we found evidence for an estrogen receptor (ER)–mediated inhibition of the NF-κB signaling pathway. NF-κB target genes were significantly elevated in ER− versus ER+ breast tumors. Also, the amount of immunostained nuclei for RelB ($P = 0.025$) and NFkB1 ($P = 0.031$) was higher in ER− breast tumors versus ER+ breast tumors.

Conclusions: The NF-κB transcription factor pathway probably contributes to the phenotype of IBC and possibly offers new options for treatment of patients diagnosed with this aggressive form of breast cancer.

Authors' Affiliations: [1]Translational Cancer Research Group (Laboratory of Pathology, University of Antwerp and Oncology Center, General Hospital Sint-Augustinus); [2]Department of Epidemiology and Social Medicine, University of Antwerp, Wilrijk, Belgium; and [3]Cancer Research UK Growth Factor Group, Weatherall Institute of Molecular Medicine, John Radcliffe Hospital, Oxford, United Kingdom

Received 12/22/05; revised 3/15/06; accepted 3/28/06.

The costs of publication of this article were defrayed in part by the payment of page charges. This article must therefore be hereby marked *advertisement* in accordance with 18 U.S.C. Section 1734 solely to indicate this fact.

Requests for reprints: Peter B. Vermeulen, Department Pathology-AZ Sint-Augustinus, Oosterveldlaan 24, B2610 Wilrijk, Belgium. Phone: 323-443-52-39; Fax: 323-443-30-36; E-mail: Peter.Vermeulen@GVAgroup.be.

doi:10.1158/1078-0432.CCR-05-2800

Breast cancer is the most frequent cancer in women and represents the second leading cause of cancer death among women (1, 2). Inflammatory breast cancer (IBC) is a distinct clinical subtype of locally advanced breast cancer, with a particularly aggressive behavior and poor prognosis. Clinically, IBC typically presents with rapidly progressive breast erythema, warmth, edema, and induration (3). At the time of diagnosis, most patients have axillary lymph node involvement and one of three of the patients have metastasis in distant organs (4, 5). The characteristic pathology is the invasion of dermal lymphatics by tumor emboli; however, this is only present in 50% to 75% of the cases (4–6). Hence, IBC is primarily a

clinical diagnosis classified as T4d in the tumor-node-metastasis classification of the American Joint Committee on Cancer (7). Despite advances in multidisciplinary treatment, the prognosis of IBC is less favorable than of non-IBC, with a 3-year survival of ~40% (4).

Recently, both *in vitro* and *in vivo* experiments have indicated that the biology of IBC has some important differences with the biology of other breast carcinomas. Overexpression of the RhoC GTPase (8–11) and loss of WISP3 protein expression (9, 11) are highly correlated with the IBC phenotype. It has been shown that overexpression of the RhoC GTPase is directly and specifically implicated in the production of angiogenic factors by IBC cells (12). In human samples, increased angiogenesis in IBC was evident by both an increased number of microvessels and a higher fraction of proliferating endothelial cells (13), as well as increased expression of several angiogenic growth factors and growth factor receptors in IBC compared with non-IBC (14). The specific biology of IBC was further shown by the fact that a molecular signature based on the differential expression of 756 genes is able to separate IBC from non-IBC in an unsupervised hierarchical clustering analysis. The 756 gene–based molecular signature was subjected to a detailed analysis, revealing the presence of several nuclear factor-κB (NF-κB) target genes and upstream activators of the NF-κB signaling pathway, with strong expression in IBC compared with non-IBC (15).

The aim of the present study was to confirm the contribution of the NF-κB transcription factors to the molecular pathogenesis of IBC. NF-κB is a transcriptional regulator known to be involved in immunity and inflammation. In addition, NF-κB also regulates cell proliferation, apoptosis, and cell migration. The family of NF-κB transcription factors consists of five members: RelA, RelB, cRel, NFkB1, and NFkB2 (16). These proteins form various homodimers and heterodimers, which, upon activation by specific pathways, bind to DNA and induce transcription of several target genes. In the past, DNA-binding assays have been used to identify "dimerization rules": NFkB1 and NFkB2 can dimerize with all NF-κB transcription factor family members and can form homodimers. RelB and cRel do not seem to engage in homotypic interactions. RelB, furthermore, does not seem to dimerize with RelA or cRel (17). In addition, recent studies have indicated that homodimers of NFkB1 and NFkB2, or heterodimers of NFkB1 and NFkB2, lack transcriptional activity and thereby cannot induce target gene expression (17). By activating target genes, NF-κB assists in controlling several hallmarks of cancer (16, 18), two of which, (lymph-)angiogenesis and metastasis, are particularly linked to the biology of IBC.

This study shows that NF-κB is transcriptionally more active in IBC compared with non-IBC, by both gene expression assays and immunohistochemistry. This results in the induction of NF-κB target genes, possibly contributing to the molecular pathogenesis of IBC. In addition, targeted inhibition of NF-κB activation in IBC might offer new therapeutic possibilities for patients with IBC.

Materials and Methods

Patients and samples. Tumor samples were obtained from patients with breast adenocarcinoma treated at the General Hospital Sint-Augustinus (Wilrijk, Belgium). Each patient gave written informed consent. This study was approved by the local institutional review board. All samples were stored in liquid nitrogen within 15 minutes after excision (median delay of 9 minutes). Breast tumor samples included pretreatment samples of patients with IBC, diagnosed by strictly respecting the criteria mentioned in the tumor-node-metastasis classification of the American Joint Committee on Cancer as T_{4d} (7). The presence of tumor emboli was, as an isolated pathologic finding, not sufficient for the diagnosis of IBC.

RNA isolation, processing, and cDNA microarray hybridization. RNA from 16 patients with IBC and 18 patients with non-IBC ($n = 34$) was isolated and processed as described before (15) by using the RNeasy Mini kit (Qiagen, Valencia, CA). High-quality RNA was reverse transcribed, amplified, and Cy5 labeled using the Amino Ally MessageAmp aRNA kit (Ambion, Inc., Austin, TX). Universal Human Reference RNA (Stratagene, La Jolla, CA) was processed similarly and Cy3 labeled for competitive hybridization. cDNA chips were obtained from the Sanger Center and hybridized during 16 hours at 47°C in a volume of 40 μL. Information regarding the clone set and the microarray production can be obtained from the world wide web.[4] After hybridization, slides were washed and scanned immediately using ScanArray software. Data were generated using Quantarray software and analyzed using GeneSpring (Agilent Technologies, Palo Alto, CA). The methodology has been described in Van Laere et al. (15). Baseline clinicopathologic characteristics for the IBC and non-IBC patients from which samples have been used for cDNA microarray analysis are provided in Table 1.

Quantitative real-time reverse transcription-PCR. For quantitative real-time reverse transcription-PCR (RT-PCR), RNA was isolated as described before from all samples plus one additional IBC tumor and two additional non-IBC tumors ($n = 37$). One microgram of RNA from 17 IBC samples and 20 non-IBC samples in total was reverse transcribed into cDNA with random primers (High Capacity cDNA Archive kit, Applied Biosystems, Foster City, CA). PCR primers and Taqman probes for eight NF-κB target genes and two housekeeping genes were purchased as Assays-on-Demand Products for gene expression (Applied Biosystems): *vascular cell adhesion molecule 1* (*VCAM1*), *CC chemokine receptor 5* (*CCR5*), *superoxide dismutase 2* (*SOD2*), *interleukin 15* (*IL-15*), *cathepsin B* (*CTSB*), *IFN regulatory factor 7* (*IRF7*), *guanlylate-binding protein 1* (*GBP1*), *CD48 antigen* (*CD48*), *18S rRNA*, and *β-actin*. *18S rRNA* and *β-actin* were used as housekeeping genes to control for reverse transcriptase efficiency, RNA degradation, PCR inhibition, and RNA input. Human Universal Reference RNA (Stratagene) was used as calibrator to calculate relative gene expression for the above mentioned genes. Quantitative real-time RT-PCR was done on the ABI 7700 Sequence Detector (Applied Biosystems). All PCR reactions were done in duplicate. Relative gene expression was calculated with the $2^{-\Delta\Delta Ct}$ method (19) as described before (14). Baseline clinicopathologic characteristics for the IBC and non-IBC patients from which samples have been used for RT-PCR analysis are provided in Table 1.

Immunohistochemistry. Antibodies purchased from Santa Cruz Biotechnology (Santa Cruz, CA) were used for immunohistochemical staining of RelA (clone C-20), RelB (clone C-19), NFkB1 (clone C-19), NFkB2 (clone K-27), and cRel (clone B-6). Formalin-fixed, paraffin-embedded tissue sections from 44 IBC tumors and 46 non-IBC tumors, including the samples used for cDNA microarray analysis and quantitative real-time RT-PCR, were rehydrated through sequential changes of alcohol and distilled water. Antigen retrieval was done for 30 minutes in citrate buffer (pH 6) for RelA, RelB, NFkB1, and NFkB2 at 95°C. For cRel, antigen retrieval was done for 30 minutes in Tris-EDTA buffer (pH 9) at 95°C. Sections were incubated for 1 hour at room temperature using a dilution of 0.2, 4.0, 1.3, 2.7, and 2.0 μg/mL, respectively. The DAKO Envision system on the DAKO Cytomation

[4] www.sanger.ac.uk/Projects/Microarrays.

Table 1. Clinicopathologic characteristics for patients with IBC and non-IBC used for immunohistochemistry, RT-PCR, cDNA microarray, and NF-κB DNA-binding experiments

	Immunohistochemistry (n = 90)		PCR (n = 37)		cDNA array (n = 34)		DNA-binding assays (n = 17)	
	Non-IBC (n = 46)	IBC (n = 44)	Non-IBC (n = 20)	IBC (n = 17)	Non-IBC (n = 18)	IBC (n = 16)	Non-IBC (n = 10)	IBC (n = 7)
Age (y)								
Median (range)	59 (33-81)	59 (33-83)	61 (42-78)	56 (41-74)	61 (42-78)	56 (41-74)	62 (33-78)	56 (49-74)
Histologic type								
Ductal	39	41	18	15	16	14	10	7
Lobular	7	3	2	2	2	2	0	0
Tumor emboli in dermal lymph vessels								
Present	8	28	2	14	2	13	3	4
Absent	38	16	18	3	16	3	7	3
Grade*								
1	11	0	6	0	5	0	3	0
2	25	20	8	8	8	7	3	3
3	10	24	6	9	5	9	4	4
T stadium								
1	14	0	6	0	5	0	2	0
2	11	0	4	0	3	0	4	0
3	10	0	7	0	7	0	3	0
4	11	44	3	17	3	16	1	7
N stadium†								
0	19	1	8	0	7	0	2	0
1	24	16	11	6	10	5	7	1
2	3	27	1	11	1	11	1	6
ER status‡								
ER−	17	32	11	13	9	12	7	5
ER+	29	12	9	4	9	4	3	2
PR status§								
PR−	20	34	11	13	8	12	7	2
PR+	26	10	9	4	10	4	3	5

*According to the Elston-Ellis modification of the SBR grading system.
†The N stadium for patients with IBC was determined clinically.
‡ER status was determined using the anti-ER antibody (clone 1D5) and a cutoff level of 10% to discriminate between the absence or presence of nuclear protein expression.
§PR status was determined using the anti-PR antibody (clone PgR636) and a cutoff level of 10% to discriminate between the absence or presence of nuclear protein expression.

autostainer was used for visualization of the antibody binding. Tissue sections were counterstained using hematoxylin and mounted for light microscopy. In each tissue section, hotspots with nuclear staining were searched for and within these hotspots a total number of 500 nuclei was counted at a magnification of ×400. Baseline clinicopathologic characteristics for the IBC and non-IBC patients from which samples have been used for immunohistochemical analysis are provided in Table 1.

NF-κB DNA-binding assays. To evaluate NF-κB DNA-binding in IBC and non-IBC samples, we extracted nuclear proteins from 7 IBC and 10 non-IBC patients of whom sufficient tumor tissue was left. Baseline clinicopathologic characteristics for the IBC and non-IBC patients from which samples have been used for NF-κB DNA-binding assays are provided in Table 1. Nuclear extraction was done with the Nuclear Extract kit (Active Motif, Carlsbad, CA) according to the protocol of the manufacturer. Briefly, at least 200 mg of each tissue were pulverized in liquid nitrogen. After addition of a hypotonic buffer, supplemented with 1 mol/L DTT and detergent, tissue was homogenized. The suspension was incubated on ice during 15 minutes followed by a centrifugation at 4°C during 10 minutes at 850 × g to pellet single cells. Single cells were then resuspended in hypotonic buffer, supplemented with detergent, to permeabilize the cell membranes and extract the cytoplasmic proteins and nuclei. The suspension was incubated on ice during 15 minutes. Nuclei were collected by centrifuging the suspension at 14,000 × g in a precooled centrifuge at 4°C during 30 seconds. After removal of the supernatants, containing cytoplasmic proteins, the pellet was again resuspended in a lysis buffer, supplemented in 1 mol/L DTT, to break down the nuclei and extract the nuclear proteins. Suspension was incubated on ice during 30 minutes on a rocking platform at 150 rpm, after which nuclear proteins were collected by centrifuging the suspension at 14,000 × g in a precooled centrifuge at 4°C during 10 minutes. Protein concentration was determined using a bicinchoninic acid protein assay. The supernatant was stored at −80°C until used to determine NF-κB DNA-binding within each sample.

NF-κB DNA-binding for each NF-κB family member was evaluated using the ELISA-based TransAM NF-κB Family kit (Active Motif)

following the protocol of the manufacturer. In these commercial kits, a duplexed NF-κB oligonucleotide containing a κB consensus sequence is attached to the surface of 96-well plates. Activated NF-κB dimers in 20 μg nuclear extract bound to the attached oligonucleotide is specifically and quantitatively detected by subsequent incubation with antibodies against the activated forms of RelA, RelB, cRel, NFkB1, and NFkB2, followed by an enzyme-linked (horseradish peroxidase) secondary antibody for colorimetric scoring. The absorbance was measured on an ELISA reader at 450 nm with a reference wavelength of 655 nm.

Statistical analysis. Statistical analysis was done with the SPSS software (version 12.0, SPSS, Inc., Chicago, IL). Differences in relative gene expression for the NF-κB target genes between IBC and non-IBC or differences in NF-κB DNA-binding between IBC and non-IBC were analyzed for significance using a Mann-Whitney *U* test. Correlations between relative gene expression data of different genes were calculated using Spearman correlation coefficients. Differences in nuclear protein expression for the NF-κB transcription factor family members were analyzed for significance with a Mann-Whitney *U* test. Correlations between immunohistochemical results for each NF-κB family member and NF-κB DNA-binding for each family member were investigated by calculating Spearman correlation coefficients. To investigate the contribution of each of the transcriptionally active NF-κB dimers to the distinction between IBC and non-IBC, we did a logistic regression with the transcriptionally active NF-κB dimers as independent variables and the tumor phenotype as dependent variable. Correlations between immunohistochemical results and estrogen receptor (ER) status were studied using a Fisher's exact test or a χ^2 test. Differences in relative gene expression for the NF-κB target genes related to ER status were analyzed for significance using a Mann-Whitney *U* test.

Results

NF-κB target gene expression by cDNA microarrays and real-time RT-PCR in IBC versus non-IBC. Out of the list of differentially expressed NF-κB target genes with a statistically significant overexpression in IBC (n = 28), we selected eight genes for validation by quantitative real-time RT-PCR based on a 3-fold overexpression in the IBC group compared with the non-IBC group (15): *VCAM1*, *CCR5*, *SOD2*, *IL-15*, *CTSB*, *IRF7*, *GBP1*, and *CD48*. Relative gene expression differences measured by real-time RT-PCR (17 IBC and 20 non-IBC) and cDNA microarrays (16 IBC and 18 non-IBC) for eight different NF-κB target genes are summarized in Table 2. For IBC and non-IBC, the minimum, median, and maximum relative gene expression values are reported for the above-mentioned genes in each analysis. Median relative gene expression levels for all NF-κB target genes are elevated in IBC compared with non-IBC, independent of the analysis method. For most NF-κB target genes, except *IL-15*, the difference in gene expression reached significance. For *IL-15*, a trend toward a significant overexpression in IBC was observed by both cDNA microarray analysis and real-time RT-PCR.

Gene expression data for NF-κB target genes measured by cDNA microarrays and real-time RT-PCR were significantly correlated with each other in 22 of 28 comparisons (significant correlation coefficients ranging from 0.326 to 0.788) and 27 of 28 comparisons (significant correlation coefficients ranging from 0.379 to 0.879), respectively, indicating a common transcriptional regulation for all NF-κB target genes. For six of eight NF-κB target genes, gene expression data measured by cDNA microarrays and real-time RT-PCR significantly correlated with each other: *VCAM1* (R_s = 0.602, $P < 0.001$), *CCR5* (R_s = 0.546, P = 0.001), *IL-15* (R_s = 0.366, P = 0.046), *CTSB* (R_s = 0.349, P = 0.047), *GBP1* (R_s = 0.609, $P < 0.001$), and *CD48* (R_s = 0.438, P = 0.004). For *SOD2* and *IRF7*, no significant correlation was found.

Immunohistochemistry for different NF-κB transcription factor family members. To further elucidate the contribution of the NF-κB transcription factor family to the IBC phenotype,

Table 2. Relative gene expression differences measured by real-time RT-PCR and cDNA microarrays for eight different NF-κB target genes

	VCAM1	CCR5	SOD2	IL-15	CTSB	IRF7	GBP1	CD48
Real-time RT-PCR								
IBC								
Minimum	1.268	0.309	0.594	0.369	0.559	0.467	2.132	0.194
Median	3.706	6.375	1.627	1.322	1.641	2.727	8.383	2.657
Maximum	15.322	29.446	7.464	32.167	9.714	21.185	78.521	31.945
Non-IBC								
Minimum	0.292	0.194	0.211	0.118	0.423	0.268	0.503	0.191
Median	1.258	1.836	0.519	0.742	0.918	1.396	2.729	1.396
Maximum	17.03	14.197	2.612	7.768	2.313	9.815	15.032	8.084
P	0.001	0.003	0.001	0.069	0.002	0.020	0.002	0.001
cDNA microarray analysis								
IBC								
Minimum	1.306	0.395	0.776	0.395	0.871	0.777	0.904	0.721
Median	2.956	1.780	1.178	1.458	1.578	1.060	2.319	1.487
Maximum	4.895	7.240	1.951	2.839	3.090	1.352	6.368	4.205
Non-IBC								
Minimum	0.254	0.454	0.360	0.553	0.596	0.651	0.422	0.717
Median	1.584	1.251	1.016	1.028	1.131	0.911	1.600	1.107
Maximum	4.195	2.035	1.479	2.774	2.423	1.311	3.157	1.552
P	0.01	0.006	0.010	0.053	0.011	0.007	0.007	0.012

immunohistochemistry for RelA, RelB, cRel, NFkB1, and NFkB2 was executed on tissue sections from 44 IBC specimens and 46 non-IBC specimens. A significant difference in amount of stained nuclei from tumor cells was found for RelB ($P = 0.038$) and NFkB1 ($P < 0.001$) with a higher median value for the number of stained tumor cell nuclei in IBC (RelB, 36.20% positive nuclei; NFkB1, 67.90% positive nuclei) compared with non-IBC (RelB, 0.00% positive nuclei; NFkB1, 50.00% positive nuclei). For RelA, cRel, and NFkB2, no statistical difference was found. An important observation was the fact that not only tumor cells but also stromal cells stained using different NF-κB antibodies. Figure 1 shows tissue sections with and without nuclear staining using antibodies against RelA, RelB, cRel, NFkB1, and NFkB2. On the left, tissue sections of breast tumors with pronounced nuclear staining are displayed. On the right, tissue sections of breast tumors with cytoplasmic staining are displayed (×400 magnification).

Transcriptionally active NF-κB only consists of specific homodimers or heterodimers (16, 17). Therefore, we investigated if transcriptionally active NF-κB dimers are present more often in IBC compared with non-IBC. For that purpose, we dichotomized the percentage of stained nuclei counted in each tissue section for each NF-κB transcription factor family member according to a cutoff value of 50%. Then, for each patient, we looked for transcriptionally active combinations of NF-κB family members, taking into account the dimerization rules and the fact that homodimers of NFkB1 or NFkB2 or the heterodimer NFkB1/NFkB2 are transcriptionally inactive (17). When transcriptionally active NF-κB dimers were identified within a tissue section, the tumor was considered immunohistochemically positive for NF-κB. Hence, we identified 19 of 44 IBC specimens with transcriptionally active NF-κB dimers compared with only 2 of 46 non-IBC specimens with transcriptionally active NF-κB dimers (Pearson χ^2, $P < 0.001$). These results clearly show that NF-κB is more often activated in IBC compared with non-IBC as was evident from the identification of the NF-κB target gene signature in a list of 756 genes differentially expressed between IBC and non-IBC. To further validate this approach, we compared NF-κB target gene expression in breast tumors with and without transcriptionally active NF-κB present in the tumor cells. We found statistically significant differences in relative gene expression for five of eight NF-κB target genes (*VCAM1*, $P = 0.050$; *CCR5*, $P = 0.019$; *SOD2*, $P = 0.013$; *IRF7*, $P = 0.050$; and *CTSB*, $P = 0.012$) and trends toward a statistical significant difference in relative gene expression for two of eight NF-κB target genes (*GBP1*, $P = 0.056$; *CD48*, $P = 0.073$), with higher median relative gene expression levels in the group with NF-κB-positive breast tumors. When using lower cutoff values (e.g., 30% and 40%) to discriminate between the presence and the absence of individual NF-κB transcription factors, similar results were obtained, indicating that our results are valid independent of the chosen cutoff value.

To investigate the contribution of the individual transcriptionally active NF-κB dimers to the IBC and non-IBC phenotype, we did a conditional backward logistic regression with the different transcriptionally active NF-κB dimers as independent variables and the IBC or non-IBC phenotype as dependent variable. The RelB/NFkB1 dimer was identified as the most predictive dimer to discriminate IBC from non-IBC ($\beta = 2.4$; $P = 0.003$). Using a model based on the RelB/NFkB1 dimer, we were able to correctly predict 66.3% of the IBC and non-IBC specimens in our data set of 44 IBC and 46 non-IBC specimens. The RelB/NFkB1 dimer was also identified as most discriminating dimer using lower cutoff values, indicating that our results are valid independent of the chosen cutoff values.

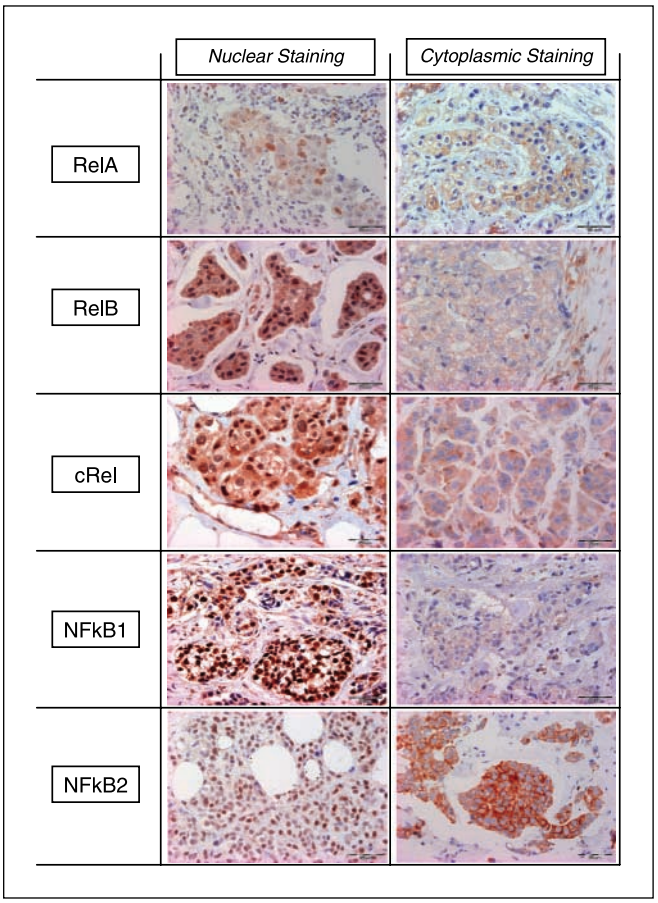

Fig. 1. Nuclear and cytoplasmic staining of breast tumor tissue sections using antibodies against all different NF-κB family members.

NF-κB DNA-binding in IBC versus non-IBC. When comparing NF-κB DNA-binding in 7 IBC and 10 non-IBC samples, we found non-significantly elevated median NF-κB DNA-binding for all NF-κB transcription factor family members. We argue that this observation is due to a small sample size. Most of the tissue of the IBC and non-IBC samples has been used to extract RNA from for both cDNA microarray analysis and quantitative real-time RT-PCR. Therefore, for most IBC and non-IBC samples under study, few amounts of tissue were left over to perform NF-κB DNA-binding experiments with. Only those samples with at least 200 μg of tissue leftover were selected to extract nuclear proteins from and determine NF-κB DNA-binding. Results from the NF-κB DNA-binding experiments are displayed in a box-and-whisker plot (Fig. 2).

The NF-κB DNA-binding correlated significantly with the percentage of stained nuclei for three of five NF-κB family members: RelA ($R_s = 0.481$, $P = 0.050$), RelB ($R_s = 0.707$, $P = 0.001$), and NFkB1 ($R_s = 0.767$, $P = 0.001$). For NFkB2, a trend toward a significant correlation was found between NFkB2 DNA-binding and the percentage of NFkB2-stained nuclei ($R_s = 0.440$, $P = 0.058$). The correlations between NF-κB

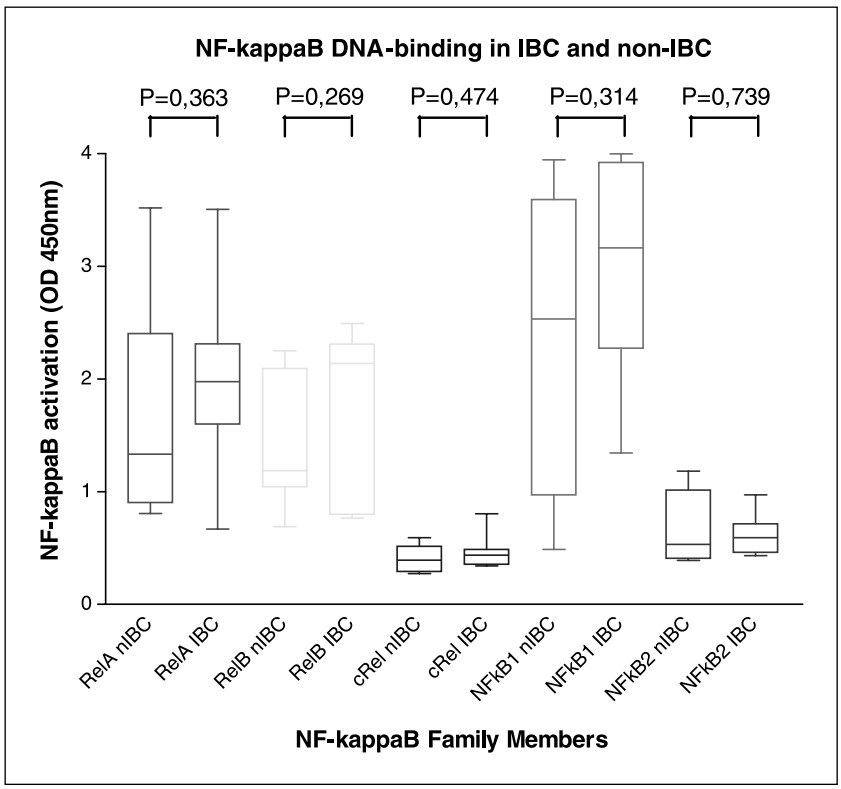

Fig. 2. Comparison of NF-κB DNA-binding data between IBC and non-IBC for each NF-κB family member.

DNA-binding and the percentage of stained nuclei for four of five NF-κB transcription factor family members validate our immunohistochemical data. Next, we analyzed whether a difference in NF-κB target gene expression was observed between samples with transcriptionally active NF-κB bound to DNA. Therefore, we dichotomized the absorption values that correlate with NF-κB DNA-binding to the median absorption value for each NF-κB transcription factor family member. Then, we looked for transcriptionally active NF-κB dimers bound to DNA by taking into account the dimerization rules and the fact that homodimers of NFkB1 or NFkB2 or the heterodimer NFkB1/NFkB2 are transcriptionally inactive (17). All NF-κB target genes showed elevated median relative gene expression in the group with transcriptionally active NF-κB dimers bound to DNA. Four of eight NF-κB target genes with an elevated median relative gene expression in the group with transcriptionally active NF-κB bound to DNA showed significant differences in relative gene expression level: *SOD2* ($P = 0.008$), *CTSB* ($P = 0.043$), *GBP1* ($P = 0.008$), and *CCR5* ($P = 0.008$). One of eight NF-κB target genes with an elevated median relative gene expression level in the group of tumors with transcriptionally active NF-κB bound to DNA showed a trend toward a significant difference in relative gene expression level: *IL-15* ($P = 0.058$). For *VCAM1*, *IRF7*, and *CD48*, no significant difference was found ($P = 0.133$, $P = 0.170$, and $P = 0.212$, respectively), although median relative gene expression level was elevated in the group of breast tumors with transcriptionally active NF-κB dimers bound to DNA.

Correlations with ER status. We investigated the inverse relationship between NF-κB activation, measured by immunohistochemistry, in clinically ER+ versus ER− breast tumor specimens. We found a significant difference between immunohistochemical ER+ and immunohistochemical ER− groups for RelB ($P = 0.025$) and NFkB1 ($P = 0.031$), with a higher median percentage of positive nuclei in immunohistochemical ER− versus immunohistochemical ER+ groups for RelB and NFkB1. Transcriptionally active NF-κB dimers were identified in 16 of 49 immunohistochemical ER− tumors. In the immunohistochemical ER+ group, only 3 of 41 breast tumors with transcriptionally active NF-κB dimers were identified ($\kappa = -0.251$; $P < 0.0001$). When analyzing relative gene expression differences for NF-κB target genes, measured by real-time RT-PCR, between immunohistochemical ER+ versus immunohistochemical ER− breast tumor specimens, we found a significant increase in relative gene expression level for four of eight NF-κB target genes (*SOD2*, *CD48*, *VCAM1*, and *GBP1*) with median relative gene expression levels higher in immunohistochemical ER− breast tumors for all NF-κB target genes. For three of eight NF-κB target genes (*IRF7*, *CTSB*, and *CCR5*), a trend toward a significant increase in relative gene expression levels in the immunohistochemical ER− tumors compared with the immunohistochemical ER+ tumors was observed. Results are displayed in Fig. 3. Values in the scatter plot are relative gene expression levels for all NF-κB targets.

Discussion

According to Hannahan and Weinberg (18), tumorigenesis requires six essential alterations to normal cell physiology: self-sufficiency in growth signals, insensitivity to growth inhibition, evasion of apoptosis, immortalization, sustained angiogenesis, and tissue invasion and metastasis. Recently, it has been shown that most of the above-mentioned aspects of tumorigenesis are more active in IBC compared with non-IBC.

For example, an unbiased analysis of genes differentially expressed between IBC and non-IBC has revealed the importance of metastasis-related processes and cell proliferation for the biology of IBC (15) and several independent studies have proven the importance of (lymph-)angiogenesis in IBC, both *in vitro* and *in vivo* (13, 14, 20). The importance of the NF-κB transcription factor for some of the tumor-related processes more active in IBC suggests that NF-κB might be a key player in the development of IBC as well as a potential therapeutic target. In this context, a logistic regression model, using the different transcriptional active NF-κB dimers as independent variables and the tumor phenotype (IBC or non-IBC) as dependent variable, is able to assign up to 66.3% of the samples in our data set of 44 IBC and 46 non-IBC specimens to the correct class, indicating the importance of the NF-κB transcription factor family for the tumor cell biology of IBC.

Taking into account the fact that IBC is more often hormone receptor negative than non-IBC and the fact that the prevalence of the ErbB2 amplification is elevated in IBC compared with non-IBC (10), the increased activation of NF-κB in IBC compared with non-IBC is consistent with previously published research on NF-κB activation in human breast cancer and in breast cancer cell lines (21, 22). Biswas et al. (21, 22) reported that NF-κB is activated more often in ER− human breast tumors compared with ER+ human breast tumors, and most predominantly in ER− and ErbB2+ breast tumors. The observation that NF-κB is more often activated in ER− breast tumors suggests an inhibition of the NF-κB signaling pathway by ER. In breast cancer, Zhou et al. (23) studied the activation of NF-κB in two groups of ER+ breast tumors. Early-stage primary breast cancers selected for lower ER content showed 2- to 4-fold increased NFkB1 and RelA DNA-binding over a second set of primary breast cancers with higher ER content. This shows that the level of NF-κB activation is inversely correlated with ER content. From a clinical point of view, the negative interaction between the NF-κB and ER pathways is also evident. The malignant progression of some breast cancers is coincident with a shift from estrogen dependence to estrogen independence. This shift coincides with an increase in both NF-κB DNA-binding activity (24, 25) and expression of NF-κB target genes like IL-8 (26). Some breast tumors that are resistant to the tumoricidal effect of antiestrogens, such as tamoxifen, become sensitized to apoptosis and show a reduction in NF-κB activity after treatment with estrogen. This suggests that the proapoptotic effects of estrogen in these tumors are mediated through inhibition of NF-κB (27). ER has been shown to block NF-κB activity at several steps: (*a*) it can inhibit the IKK activity; (*b*) it can inhibit degradation of IκB; (*c*) it can block DNA-binding by NF-κB; (*d*) it can bind coactivators and compete with NF-κB for coactivator binding; and (*e*) it can directly bind to DNA-bound NF-κB to inhibit NF-κB-mediated transcriptional activation (28). In addition, the cross-coupling between ER and NF-κB also results in reduced activity of promoters with ER binding sites (29). In our study, the inhibitory interaction between ER and NF-κB transcription factors was evident from a significant increase in NF-κB target gene expression in ER− tumors, as well as a significantly elevated amount of transcriptionally active NF-κB dimers in ER− tumors compared with ER+ tumors. Furthermore, for RelB and NFkB1, we found a significantly elevated amount of stained nuclei in ER− breast

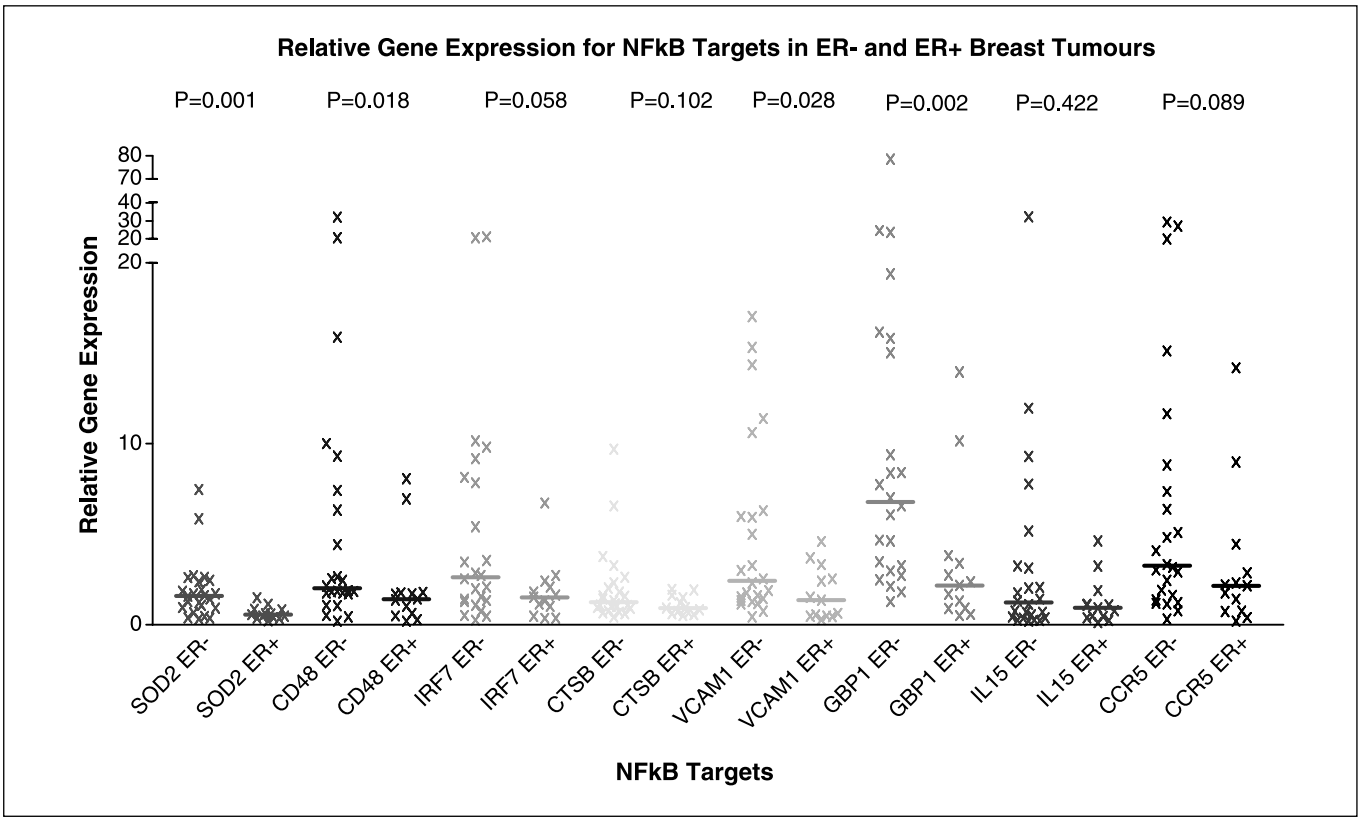

Fig. 3. Median relative NF-κB target gene expression level in clinically ER+ and ER− breast tumor specimens.

tumors compared with ER+ breast tumors. The fact that the frequency of ER− IBC tumors is higher compared with non-IBC tumors could explain the increased NF-κB activation in IBC compared with non-IBC.

In ER− and ErbB2− breast tumors, nuclear NF-κB was detected mostly in stroma, suggesting a role for activated NF-κB in intercellular signaling between epithelial and stromal cells (21, 22). The possible contribution of stromal NF-κB activation to the NF-κB signature of IBC cannot be ruled out. Due to the growth pattern of IBC tumors, the stromal component in IBC is more pronounced compared with non-IBC, as was evidenced by a significant difference in tumor/stroma ratio between IBC and non-IBC tumors (15). Therefore, increased activity of NF-κB, measured by real-time RT-PCR and cDNA microarrays for NF-κB target genes in IBC, can be explained alternatively. One might reason that the expression of NF-κB target genes in stromal cells, like endothelial and inflammatory cells, contributes to the differential expression pattern of NF-κB target genes between IBC and non-IBC tumors. Because angiogenesis and lymphangiogenesis are processes more activated in IBC compared with non-IBC, the possibility that endothelial expression of NF-κB target genes contributes to the NF-κB signature of IBC cannot be ruled out. In this context, the expression of Prox-1, a marker for lymphatic endothelial cells (14), measured by real-time RT-PCR significantly correlated with the expression of seven of eight NF-κB target genes (data not shown). This is indicative for the fact that stroma probably contributes to the NF-κB signature of IBC. In addition, we observed that lymphatic endothelial cell proliferation was significantly elevated in NF-κB immunohistochemically positive versus NF-κB immunohistochemically negative tumors, for both IBC and non-IBC tumors (data not shown). However, the expression of NF-κB targets differs significantly between tumors with and without tumor cells, and not stromal cells, with transcriptionally active NF-κB by immunohistochemistry, thereby indicating that tumor cells are the main source of NF-κB target gene expression.

In conclusion, the NF-κB signature of IBC offers an explanation for the inflammatory symptoms because NF-κB is an activator of several inflammatory genes. Moreover, the activation of NF-κB can explain several aspects of IBC tumor biology. Due to induction of several chemotactic genes, as well as growth factors, angiogenic factors, and matrix metalloproteinases, NF-κB can be responsible for metastasis, cell proliferation, and angiogenesis, processes known to belong to the biology of IBC more than of non-IBC. The activation of NF-κB in IBC also provides a novel molecular target for treatment of patients with IBC, and potentially of ER− breast cancer in general. Studies with inhibitors of NF-κB, like Bortezomib, a proteasome inhibitor, are ongoing. Additionally, cell line experiments will be carried out to further investigate the contribution of NF-κB activation to the IBC phenotype.

References

1. Dumitrescu RG, Cotarla I. Understanding breast cancer risk—where do we stand in 2005? J Cell Mol Med 2005;9:208–21.
2. Key TJ, Verkasalo PK, Banks E. Epidemiology of breast cancer. Lancet Oncol 2001;2:133–40.
3. Haagensen CD. Inflammatory carcinoma. In: Haagensen CD, editor. Diseases of the breast. Philadelphia: WB Saunders; 1956. p. 488–98.
4. Lerebours F, Bieche I, Lidereau R. Update on inflammatory breast cancer. Breast Cancer Res 2005;7:52–5.
5. Kleer CG, Van Golen KL, Merajver SD. Molecular biology of breast cancer metastasis. Inflammatory breast cancer: clinical syndrome and molecular determinants. Breast Cancer Res 2000;2:423–9.
6. Low JA, Berman AW, Steinberg SM, Danforth DN, Lippman ME, Swain SM. Long-term follow-up for locally advanced and inflammatory breast cancer patients treated with multimodality therapy. J Clin Oncol 2004;22:4067–74.
7. Singletary SE, Allred C, Ashley P, et al. Revision of the American Joint Committee on Cancer staging system for breast cancer. J Clin Oncol 2002;17:3628–36.
8. Van Golen KL. Inflammatory breast cancer: relationship between growth factor signaling and motility in aggressive cancers. Breast Cancer Res 2003;5:174–9.
9. Van Golen KL, Davies S, Wu ZF, et al. A novel putative low-affinity insulin-like growth factor binding protein, LIBC (lost in inflammatory breast cancer), and RhoC GTPase correlate with the inflammatory breast cancer phenotype. Clin Cancer Res 1999;5:2511–9.
10. Van den Eynden GG, Van der Auwera I, Van Laere S, et al. Validation of a tissue microarray to study differential protein expression in inflammatory and non-inflammatory breast cancer. Breast Cancer Res Treat 2004;85:13–22.
11. Kleer CG, Zhang Y, Pan Q, et al. WISP3 and RhoC guanosine triphosphatase cooperate in the development of inflammatory breast cancer. Breast Cancer Res 2004;6:R110–5.
12. Van Golen KL, Wu ZF, Qiao XT, Bao L, Merajver SD. RhoC GTPase overexpression modulates induction of angiogenic factors in breast cells. Neoplasia 2000;2:418–25.
13. Colpaert CG, Vermeulen PB, Benoy I, et al. Inflammatory breast cancer shows angiogenesis with high endothelial proliferation rate and strong E-cadherin expression. Br J Cancer 2003;88:718–25.
14. Van der Auwera I, Van Laere SJ, Van den Eynden GC, et al. Increased angiogenesis and lymphangiogenesis in inflammatory versus noninflammatory breast cancer by real-time reverse transcriptase-PCR gene expression quantification. Clin Cancer Res 2004;10:7965–71.
15. Van Laere SJ, Van der Auwera I, Van den Eynden GG, et al. Distinct molecular signature of inflammatory breast cancer by cDNA microarray analysis. Breast Cancer Res Treat 2005;3:237–46.
16. Karin M, Cao Y, Greten FR, Li ZW. NF-kB in cancer: from innocent bystander to major culprit. Nat Rev Cancer 2002;2:301–10.
17. Hoffmann A, Leung TH, Baltimore D. Genetic analysis of NF-kB/Rel transcription factors defines functional specificities. EMBO J 2003;22:5530–9.
18. Hanahan D, Weinberg RA. The hallmarks of cancer. Cell 2000;100:57–70.
19. Livak KJ, Schmittgen TD. Analysis of relative gene expression data using real-time quantitative PCR and the $2(-\Delta\Delta C(T))$ method. Methods 2001;25:402–8.
20. Van der Auwera I, Van den Eynden GG, Colpaert CG, et al. Tumor lymphangiogenesis in inflammatory breast carcinoma: a histomorphometric study. Clin Cancer Res 2005;11:7637–42.
21. Biswas DK, Dai SC, Cruz A, Weiser B, Graner E, Pardee AB. The nuclear factor κB (NF-κB): a potential therapeutic target for estrogen receptor negative breast cancers. Proc Natl Acad Sci U S A 2001;98:10386–91.
22. Biswas DK, Cruz AP, Gansberger E, Pardee AB. Epidermal growth factor-induced nuclear factor κB activation: a major pathway of cell-cycle progression in estrogen-receptor negative breast cancer cells. Proc Natl Acad Sci U S A 2000;97:8542–7.
23. Zhou Y, Eppenberger-Castori S, Marx C, et al. Activation of nuclear factor-κB (NFκB) identifies a high-risk subset of hormone-dependent breast cancers. Int J Biochem Cell Biol 2005;37:1130–44.
24. Pratt MA, Bishop TE, White D, et al. Estrogen withdrawal-induced NF-κB activity and Bcl-3 expression in breast cancer cells: roles in growth and hormone independence. Mol Cell Biol 2003;23:6887–900.
25. Nakshatri H, Bhat-Nakshatri P, Martin DA, Goulet RJ, Sledge GW. Constitutive activation of NFκB during progression of breast cancer to hormone-independent growth. Mol Cell Biol 1997;17:3629–39.
26. Freund A, Jolivel V, Durand S, et al. Mechanisms underlying differential expression of interleukin-8 in breast cancer cells. Oncogene 2004;23:6105–14.
27. Jordan VC. Selective estrogen receptor modulation: concepts and consequences in cancer. Cancer Cell 2004;5:207–13.
28. Kalaitzidis D, Gilmore T. Transcription factor cross-talk: the estrogen receptor and NF-κB. Trends Endocrinol Metab 2005;16:46–52.
29. Stein B, Yang MX. Repression of the interleukin-6 promoter by estrogen receptor is mediated by NF-κB and C/EBPβ. Mol Cell Biol 1995;15:4971–9.

Clinical Cancer Research

Nuclear Factor-κB Signature of Inflammatory Breast Cancer by cDNA Microarray Validated by Quantitative Real-time Reverse Transcription-PCR, Immunohistochemistry, and Nuclear Factor- κB DNA-Binding

Steven J. Van Laere, Ilse Van der Auwera, Gert G. Van den Eynden, et al.

Clin Cancer Res 2006;12:3249-3256.